Available online at www.sciencedirect.com
SCIENCE DIRECT®
Bioorganic Chemistry 32 (2004) 274–289
BIOORGANIC CHEMISTRY
www.elsevier.com/locate/bioorg

Hydrophilic molecular rotor derivatives—synthesis and characterization

Mark A. Haidekker,[a,*] Thomas P. Brady,[b] Sevag H. Chalian,[b] Walter Akers,[a] Darcy Lichlyter,[a] and Emmanuel A. Theodorakis[b]

[a] *Department of Biological Engineering, University of Missouri-Columbia, Columbia, MO, USA*
[b] *Department of Chemistry and Biochemistry, University of California, San Diego, USA*

Received 22 March 2004
Available online 13 May 2004

Abstract

Recent research shows high potential for some *p*-*N*,*N*-dialkylaminobenzylidenecyanoacetates, part of a group known as fluorescent molecular rotors, to serve as fluorescent, non-mechanical viscosity sensors. Of particular interest are molecules compatible with aqueous environments. In this study, we present the synthesis and physical characterization of derivatives from 9-(2-carboxy-2-cyanovinyl)-julolidine and related molecules. All compounds show a power-law relationship of fluorescence emission with the viscosity of the solvent, different mixtures of ethylene glycol and glycerol to modulate viscosity. Compounds with high water solubility exhibit the same behavior in aqueous solutions of dextran, where the dextran concentration was varied to modulate viscosity. In addition, some compounds have been found to have low sensitivity towards changes in the pH in the physiological range. The compounds presented show promise to be used in biofluids, such as blood plasma or lymphatic fluid, to rapidly and non-mechanically determine viscosity.

1. Introduction

In biological systems, viscosity plays an important role on scales from the cellular level to the organism level. For example, cytoplasmic viscosity plays a role in cell

* Corresponding author. Fax: 1-573-884-5650.
E-mail address: HaidekkerM@missouri.edu (M.A. Haidekker).

0045-2068/$ - see front matter © 2004 Elsevier Inc. All rights reserved.
doi:10.1016/j.bioorg.2004.04.002

motion and specific lung diseases [1,2]. Cell membrane viscosity has been linked to cell mechanosensing [1,3,4], the action of anaesthetics and alcohol [5–8], and a range of diseases including atherosclerosis, cell malignancy, hypercholesterolemia, and diabetes [9–13]. On a more macroscopic level, the viscosity of body fluids, including blood plasma [14–16] and lymphatic fluid [17,18], has been linked to various disease states. In addition, the measurement and management of the appropriate blood plasma viscosity is becoming an important issue in transfusion medicine, where new strategies seeking the development of artificial blood are pursued [19–21].

The use of mechanical forces has been the primary method of measuring viscosity levels in biofluids. One type of mechanical viscometer is the cone-and-plate viscometer, where fluid is sheared between a flat plate and a cone. In this way, the resistance of the fluid to this force is measured. This is not only a time-consuming method, requiring thorough cleaning of the instrument between each measurement, but results are also influenced by artefacts, such as the formation of a protein layer at the fluid–air interface, leading to apparent non-Newtonian properties [14,22]. These drawbacks may be one reason for the limited use of viscosity measurement techniques in a clinical setting.

To overcome these limitations an alternative strategy for the measurement of viscosity has been developed based on the use of viscosity-sensitive fluorescent molecules. These compounds, commonly referred to as molecular rotors, show a well-defined relationship between fluorescence quantum yield and solvent viscosity [23]. Thus, determination of viscosity changes can be reduced to the simple measurement of fluorescence intensity [4,24–26]. In addition, fluorescence can be acquired at microscopic levels, allowing for monitoring of microviscosity [24].

For the past several years we have been engaged in the development of molecular rotors for probing the microviscosity in the lipophilic regions of the cell membrane [4,27,28]. These probes are unsuitable for use in aqueous environments due to their poor solubility. With the growing importance of viscosity measurements in aqueous solutions, we now present a group of molecular rotors that exhibit good solubility in water and can therefore be used as viscosity probes in aqueous colloid solutions and biofluids.

2. Materials and methods

2.1. General techniques

Compounds **1** (DCVJ) and **6** (CCVJ) were purchased from Helix Research (Springfield, OR). Aldehyde **7** and cyanoacetic acid methyl ester (**5e**) were purchased from Aldrich. Aldehyde **4** and compound **2e** were synthesized as previously described [28]. All reagents were commercially obtained at highest commercial quality and used without further purification. Diethyl ether (Et_2O), dichloromethane (CH_2Cl_2), toluene ($PhCH_3$), and benzene (PhH) were purified by passage through a bed of activated alumina. Yields refer to chromatographically and spectroscopically (^1H NMR, ^{13}C NMR) homogeneous materials, unless otherwise stated. Reactions were monitored by thin-layer chromatography (TLC) carried out on 0.25 mm E. Merck silica gel

plates (60F-254) using UV light as the visualizing agent and 10% ethanolic phosphomolybdic acid (PMA) or *p*-anisaldehyde solution and heat as developing agents. E. Merck silica gel (60, particle size 0.040–0.063 mm) was used for flash chromatography. Preparative thin-layer chromatography separations were carried out on 0.25 or 0.50 mm E. Merck silica gel plates (60F-254). NMR spectra were recorded on Varian Mercury 400 and/or Unity 500 MHz instruments and calibrated using the residual undeuterated solvent as an internal reference. The following abbreviations were used to explain the multiplicities: s = singlet, d = doublet, t = triplet, q = quartet, m = multiplet, and b = broad. IR spectra were recorded on a Nicolet 320 Avatar FT-IR spectrometer and values are reported in cm^{-1} units. Optical rotations were recorded on a Jasco P-1010 polarimeter and values are reported as follows: $[\alpha]_{\lambda}^{T}$ (c: g/100 ml, solvent). High resolution mass spectra (HRMS) were recorded on a VG 7070 HS mass spectrometer under chemical ionization (CI) conditions or on a VG ZAB-ZSE mass spectrometer under fast atom bombardment (FAB) conditions.

*2.2. General procedure for the preparation of α-cyanoesters **5a**, **5c**, **5d**, and **8***

To a solution of cyano acetic acid (**5**) (10 mmol), the corresponding alcohol (10 mmol) in dichloromethane (20 ml), and DMAP (1 mmol) at 0 °C was added dropwise a solution of DCC (10 mmol) in dichloromethane (10 ml). After the addition was completed, the mixture was allowed to warm to 25 °C where it was stirred for 2 h. The reaction was then diluted with dichloromethane (20 ml) and the formed DCU was filtered under gravity. The filtrate was dried ($MgSO_4$) and concentrated and the residue was purified by column chromatography (silica, 5–20% ethyl ether in hexane) to afford the corresponding esters.

*2.2.1. Ester **5a***

78% yield; colorless liquid; $R_f = 0.5$ (50% ether in hexanes); IR (film) ν_{max} 2841–2905, 2361, 1732, 1515, 1465, 1384, 1338, 1248, 1171 cm^{-1}; ^1H NMR (400 MHz, $CDCl_3$) δ 7.29 (d, $J = 8.4$ Hz, 2H), 6.89 (d, $J = 8.4$ Hz, 2H), 5.04 (s, 2H), 4.12 (t, $J = 6.8$ Hz, 2H), 3.81 (s, 3H), 3.45 (s, 2H), 2.31 (t, $J = 6.8$ Hz, 2H), 1.56 (m, 6H), 1.24 (s, 20H); ^{13}C NMR (100 MHz, $CDCl_3$) δ 173.8, 162.9, 159.4, 130.0, 128.2, 113.9, 113.0, 67.1, 65.9, 55.2, 34.3, 32.8, 29.6, 29.5, 29.4, 29.2, 29.1, 28.3, 25.6, 24.9; HRMS: Calcd for $C_{27}H_{41}NO_5$: $(M + H^+)$ 460.3063. Found 460.3089.

*2.2.2. Ester **5c***

90% yield; colorless liquid; $R_f = 0.5$ (100% ether); IR (film) ν_{max} 2886, 2252, 1746 1451, 1388, 1334, 1252, 1193, 1103 cm^{-1}; ^1H NMR (400 MHz, $CDCl_3$) δ 4.28 (m, 2H), 3.66 (m, 2H), 3.58 (m, 2H), 3.53 (m, 2H), 3.49 (s, 2H), 3.46 (q, $J = 7.2$ Hz, 2H), 1.30 (t, $J = 7.2$ Hz, 3H); ^{13}C NMR (100 MHz, $CDCl_3$) δ 163.0, 113.0, 70.2, 69.3, 68.2, 66.4, 65.4, 24.4, 14.7; HRMS: Calcd for $C_9H_{15}NO_4$: $(M + H^+)$ 202.1079. Found 202.1091.

*2.2.3. Ester **5d***

86% yield; $R_f = 0.4$ (100% ether); IR (film) ν_{max} 2886, 2252, 1746, 1451, 1388, 1334, 1252, 1193, 1103 cm^{-1}; ^1H NMR (400 MHz, $CDCl_3$) δ 4.29 (m, 2H), 3.67 (m, 2H), 3.59

(m, 6H), 3.50 (m, 2H), 3.49 (s, 2H), 3.32 (s, 3H); ^{13}C NMR (100 MHz, $CDCl_3$) δ 163.0, 113.0, 71.7, 70.4, 70.3, 68.3, 65.5, 58.8, 24.5; HRMS: Calcd for $C_{10}H_{17}NO_5$: ($M + H^+$) 232.1185. Found 232.1199.

*2.2.4. Ester **8***

74% yield; colorless liquid; $R_f = 0.5$ (90% ether in hexanes); IR (film) ν_{max} 2932–2977, 2262, 1750, 1452, 1375, 1334, 1257, 1193, 1049 cm^{-1}; ^{1}H NMR (400 MHz, $CDCl_3$) δ 4.35 (m, $J = 4.4$ Hz, 1H), 4.22 (td, $J = 4.4$ Hz, $J = 11.2$ Hz, $J = 26.4$ Hz, 2H), 4.07 (dd, $J = 6.4$ Hz, $J = 6.8$ Hz, 1H), 3.73 (dd, $J = 5.6$ Hz, $J = 6.0$ Hz, 1H), 3.51 (s, 2H), 1.40 (s, 3H), 1.33 (s, 3H); ^{13}C NMR (100 MHz, $CDCl_3$) δ 162.8, 112.8, 110.0, 109.2, 76.0, 72.9, 66.6, 65.8, 26.6, 25.1; HRMS: Calcd for $C_9H_{13}NO_4$: ($M + H^+$) 200.0923. Found 200.0931.

*2.3. General procedure for the preparation of compounds **2a**, **2c**, **2d**, **10**, and **11***

To a solution of 4-formyl julolidine (**4**) (2 mmol) and ester **5** (2 mmol) in THF (10 ml) was added DBU (2.1 mmol). After stirring at 25 °C for 1 h, the mixture was concentrated and the residue subjected to silica gel chromatography (10–50% ether in hexanes) to afford the corresponding adduct **2**.

*2.3.1. Ester **2a***

85% yield; bright orange liquid. Immediately after isolation this compound was treated with a solution of TFA/anisole (95/5) for 15 min at 25 °C. The TFA was removed under reduced pressure and the residue purified using silica gel chromatography to afford carboxylic acid **2b** (71% yield). Ester **2b**: $R_f = 0.5$ (50% ether in hexanes); IR (film) ν_{max} 2850–2923, 1701, 1560, 1519, 1316, 1230, 1162 cm^{-1}; ^{1}H NMR (400 MHz, $CDCl_3$) δ 7.94 (s, 1H), 7.51 (s, 2H), 4.25 (t, $J = 6.4$ Hz, 2H), 3.34 (t, $J = 6.0$ Hz, 4H), 2.75 (t, $J = 6.8$ Hz, 4H), 2.35 (t, $J = 7.6$ Hz, 2H), 1.96 (m, 4H), 1.75 (m, $J = 6.8$ Hz, 2H), 1.64 (m, $J = 7.2$ Hz, 2H), 1.26 (m, 22H); ^{13}C NMR (100 MHz, $CDCl_3$) δ 179.5, 164.9, 154.3, 147.6, 131.6, 120.7, 118.4, 118.0, 91.6, 65.8, 50.1, 34.0, 29.6, 29.5, 29.4, 29.2, 29.0, 28.6, 27.5, 25.8, 24.7, 21.1; HRMS: Calcd for $C_{32}H_{46}N_2O_4$: ($M + H^+$) 523.3536. Found 523.3554.

*2.3.2. Ester **2c***

78% yield; bright red oil; $R_f = 0.7$ (100% ether); IR (film) ν_{max} 2859–2931, 2207, 1705, 1614, 1565, 1519, 1442, 1316, 1230, 1161, 1098 cm^{-1}; ^{1}H NMR (400 MHz, $CDCl_3$) δ 7.88 (s, 1H), 7.45 (s, 2H), 4.36 (t, $J = 4.8$ Hz, 2H), 3.77 (t, $J = 3.6$ Hz, 2H), 3.68 (m, 2H), 3.56 (m, 2H), 3.49 (m, 2H), 3.29 (t, $J = 6$ Hz, 4H), 2.70 (t, $J = 6$Hz, 4H), 1.91 (m, $J = 6$ Hz, 4H), 1.17 (t, $J = 6.6$ Hz, 3H); ^{13}C NMR (100 MHz, $CDCl_3$) δ 164.6, 154.3, 147.6, 131.5, 120.6, 118.1, 90.9, 70.7, 69.8, 68.8, 66.5, 64.6, 50.0, 27.4, 20.9, 15.0; HRMS: Calcd for $C_{22}H_{28}N_2O_4$: ($M + H^+$) 385.2127. Found 385.2141.

*2.3.3. Ester **2d***

84% yield; bright red oil; $R_f = 0.6$ (100% ether); IR (film) ν_{max} 2859–2941, 2352, 2198, 1705, 1610, 1560, 1519, 1442, 1316, 1225, 1162, 1098 cm^{-1}; ^{1}H NMR (400 MHz,

$CDCl_3$) δ 7.92 (s, 1H), 7.49 (s, 2H), 4.39 (t, $J = 4.8$ Hz, 2H), 3.79 (t, $J = 5.2$ Hz, 2H), 3.72 (m, 2H), 3.66 (m, 4H), 3.55 (m, 2H), 3.37 (s, 3H), 3.32 (t, $J = 8.8$ Hz, 4H), 2.73 (t, $J = 6.4$ Hz, 4H), 1.95 (m, $J = 5.6$ Hz 4H); ^{13}C NMR (100 MHz, $CDCl_3$) δ 164.7, 154.5, 147.7, 131.7, 120.8, 118.4, 91.3, 71.9, 70.8, 70.6, 70.5, 68.9, 64.8, 50.1, 27.5, 21.0; HRMS: Calcd for $C_{23}H_{30}N_2O_5$: ($M + H^+$) 415.2233. Found 415.2259.

*2.3.4. Acetonide **9***

69% yield; $R_f = 0.4$ (70% ethyl ether); IR (film) ν_{max} 2937, 2207, 1703, 1619, 1565, 1513, 1439, 1311, 1229, 1157, 1098 cm^{-1}; ^{1}H NMR (400 MHz, $CDCl_3$) δ 8.08 (s, 1H), 7.92 (d, $J = 8.8$ Hz, 2H), 6.70 (d, $J = 8.8$ Hz, 2H), 4.40 (m, $J = 6$ Hz, 1H), 4.32 (m, 2H), 4.13 (dd, $J = 6$, 8.4 Hz, 1H), 3.88 (dd, $J = 5.6$, 8.4 Hz, 1H), 3.11 (s, 6H), 1.46 (s, 3H), 1.38 (s, 3H); ^{13}C NMR (100 MHz, $CDCl_3$) δ 164.1, 155.0, 153.7, 134.2, 119.3, 117.2, 111.5, 109.8, 93.2, 73.4, 66.4, 65.4, 40.0, 26.7, 25.5; HRMS: Calcd for $C_{18}H_{22}N_2O_4$: ($M + H^+$) 331.1658. Found 331.1691.

*2.3.5. Diol **10***

Compound **9** (0.5 g, 1.5 mmol) was dissolved in a mixture of THF/MeOH (1/1) and DOWEX-H^+ resin (0.10 g) was added and heterogeneous mixture was stirred for 2 h. The DOWEX-H^+ resin was removed by filtration and triethylamine (50 mg, 0.5 mmol) was added and the solvent was removed on the rotary evaporator. The residue was purified on silica gel (100% ether) to afford 200 mg of compound **10** as a bright yellow solid (46%). **10**: $R_f = 0.3$ (100% ethyl ether); IR (film) ν_{max} 3412, 2932, 2207, 1701, 1610, 1565, 1528, 1451, 1379, 1329, 1274, 1225, 1184 cm^{-1}; ^{1}H NMR (400 MHz, $CDCl_3$) δ 8.08 (s, 1H), 7.94 (d, $J = 9.2$ Hz, 2H), 6.70 (d, $J = 9.2$ Hz, 2H), 4.37 (dt, $J = 4.4$, 11.2, 23.6 Hz, 2H), 4.06 (m, $J = 4.8$ Hz, 1H), 3.74 (dt, $J = 4$, 12, 29.6 Hz, 2H), 3.13 (s, 6H); ^{13}C NMR (100 MHz, $CDCl_3$) δ 164.7, 155.1, 153.8, 134.2, 119.2, 117.6, 111.5, 92.5, 70.0, 66.7, 63.3, 40.1; HRMS: Calcd for $C_{15}H_{18}N_2O_4$: ($M + H^+$) 291.1345. Found 291.1361.

*2.3.6. Compound **11***

Compound **11** was prepared from condensation of 4-dimethylamino-benzaldehyde (**7**) (1 g, 6.7 mmol), cyano acetic acid methyl ester (0.8 g, 6.7 mmol), and DBU (1.0 g, 6.7 mmol) in 15 ml of THF as described for compound **5d**. Isolated yield: 1.4 g, 93%. **11**: $R_f = 0.4$ (50% ether in hexanes). IR (film) ν_{max} 2937, 1703, 1619, 1565, 1513, 1439, 1157, 1098 cm^{-1}; ^{1}H NMR (400 MHz, $CDCl_3$) δ 8.07 (s, 1H), 7.93 (d, $J = 8.8$ Hz 2H), 6.68 (d, $J = 8.8$ Hz, 2H), 3.88 (s, 3H), 3.10 (s, 6H); ^{13}C NMR (100 MHz, $CDCl_3$) δ 164.8, 154.7, 153.6, 134.1, 119.2, 117.6, 111.4, 93.3, 52.8, 39.9; HRMS: Calcd for $C_{13}H_{14}N_2O_2$: ($M + H^+$) 231.1133. Found 231.1156.

2.4. Spectral properties

Reagents were purchased as follows: fluoroscopy grade DMSO and dextran (87 kDa average MW) from Sigma (St. Louis, MO), ethylene glycol and glycerol from Fisher Scientific (Pittsburgh, PA). Fluorescence spectroscopy were performed in methylacrylate microcuvettes (Fisher Scientific) using Spex Fluoromax-3 (Jobin-Yvon, Stanmore, North London, UK). Based on dye solubility, a 20, 8.87 or 5 mM stock

solution in DMSO was prepared from each of the dyes listed and further diluted as needed: To determine quantum yield, the dyes were diluted to 5 μM in ethylene glycol. Mixtures of ethylene glycol (EG) and glycerol were prepared by pre-staining 5 ml of EG with 100 μl dye stock solution. One milliliter of pre-stained EG was then mixed with each 1 ml unstained EG and 8 ml glycerol, with 2 ml EG and 7 ml glycerol, with 3 ml EG and 6 ml glycerol, with 4 ml EG and 5 ml glycerol, and with 7 ml EG and 2 ml glycerol to afford solutions of different viscosity and constant dye concentration.

Since the spectral properties of each molecular rotor differs from the others, and the spectral maxima are to a small extent affected by solution polarity, the excitation and emission wavelength was examined for each dye before every experiment and optimized accordingly. Typically, 1 nm increment with 0.3 s integration and 5 nm bandwidth for excitation and emission slits was used. Peak emission intensity was calculated by averaging five data points (5 nm) centered on the peak emission.

2.5. Aqueous solutions

The aqueous solutions consisted of phosphate-buffered saline (PBS) from Sigma (St. Louis, MO) pH 7.4, with 10 μM of each dye tested. The dextran was added to make the following weight/volume solutions, 2.5, 5.0, 7.5, and 10.0%. Acid/base solutions used during pH assays consisted of distilled water; the pH was adjusted with HCl or NaOH. All solutions were calibrated and adjusted for pH before every experiment with an Oakion pH meter for accuracy.

2.6. Viscosity measurement

Viscosity was measured using a computer-controlled Brookfield DV-III+ rheometer. The viscosity was measured at ten speed settings which were determined by the percent torque on the spindle (maintained between 10 and 100%). Measurements started at 10% torque (low rpm) and were stepped up in four regular intervals to 90% torque, and measurements were subsequently repeated while stepping back down. The viscosity measurement utilized in the data is the middle step, generally 30–60% torque, as the speed was decreased back to 10% torque. Five independent measurements were taken for each solution tested and the results averaged.

3. Results

3.1. Synthesis of the molecular rotors

The general schematic of the molecular rotors analyzed can be seen in Fig. 1. The synthesis of compounds **2a**–**2e** and **10** are shown in Schemes 1 and 2, respectively. Aldehyde **4** and compound **2e** were synthesized as previously described [28]. The α-cyanoesters **5a**, **5c**, **5d**, and **8** were obtained via a dicyclohexyl carbodiimide-induced esterification of cyanoacetic acid with the corresponding alcohols in 80–95% yield. Condensation of α-cyanoesters **5** with aldehyde **4** in the presence of DBU produced

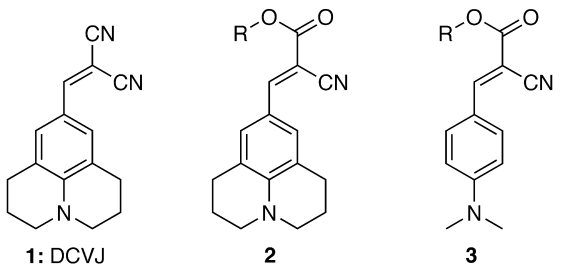

Fig. 1. General structure of the hydrophilic rotors examined (**2** and **3**) in comparison to the established dye DCVJ (**1**).

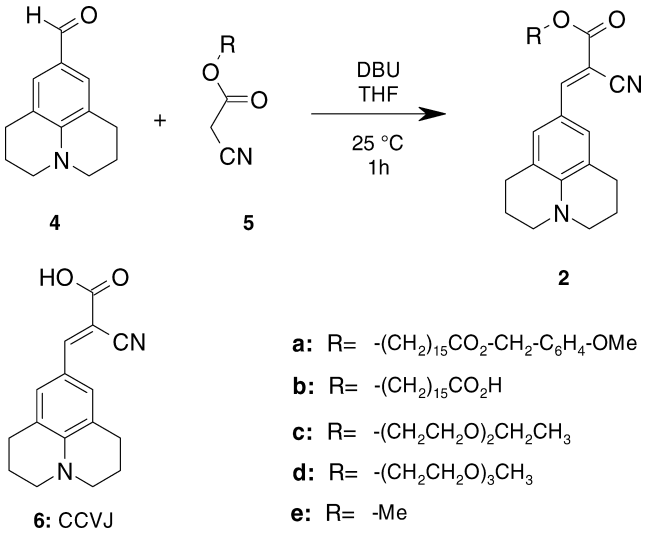

Scheme 1. Synthesis of compounds **2a**–**2e**.

the desired probes **2a**, **2c**–**2e** in very good yields (74–90%). Ester **2a** was converted to carboxylic acid **2b** upon treatment with TFA in anisole in 89% yield. In a similar manner, condensation of aldehyde **4** with ester **5e** produced compound **11**. Condensation of **4** with **8** produced compound **9** that after treatment with 1 N HCl gave rise to diol **10**. All compounds were purified by chromatography on silica gel prior to use.

3.2. Spectral properties

All molecules examined exhibited fluorescence in a similar spectral range as CCVJ. Generally, absorption was found in the blue range in the area of 420–460 nm, and emission was in the range 470–510 nm (green). Spectral maxima for all dyes are listed in Table 1. Representative excitation and emission spectra for dyes **2d**, **6**, **10**, and **11** can be seen in Fig. 2. A comparison of quantum yields was performed by measuring emission intensity and computing intensity relative to emission

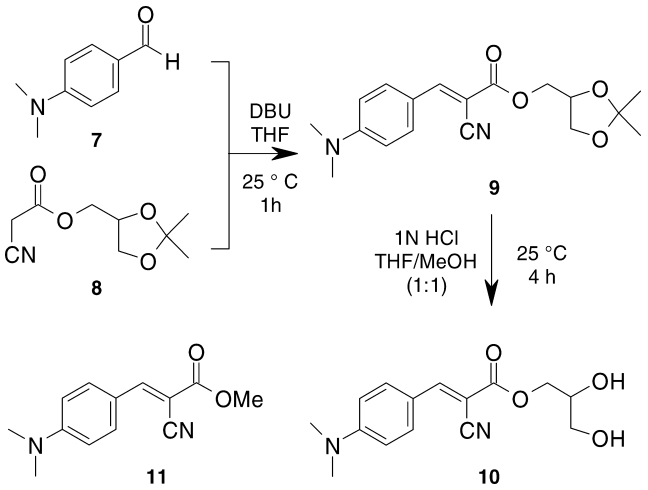

Scheme 2. Synthesis of compound **10** and structure of compound **11**.

intensity of FITC under identical conditions. In order to obtain acceptable emission signals, quantum yield comparison was performed in ethylene glycol. The relatively high viscosity of ethylene glycol elevates the emission intensity approximately by a factor of 5 over water. Table 1 lists the relative intensities of all dyes.

3.3. Water solubility

In order to obtain a qualitative evaluation of water solubility, 10 μM of each dye was dissolved in water, and the solution was tested for precipitates under the epifluorescent microscope. Dyes with high solubility showed a lower number of precipitated crystals than dyes with lower solubility, such as DCVJ. All dyes tested, including **11**, dissolved in water after less than 1 min of stirring, and did not show precipitates. The exception was **2b**, which showed few, but very large fluorescent clusters after a short time. This indicates that **2b** had limited solubility, but aggregated after a short time

Table 1
Spectral properties of the dyes analyzed

Dye	Excitation maximum (nm)	Emission maximum (nm)	Relative quantum yield in % of FITC
2b	459	502	36.0
2c	461	502	35.0
2d	460	503	28.4
10	442	485	35.7
11	440	486	27.2
1[a]	460	502	27.7
6[a]	420	486	33.8
FITC[a]	494	522	100

[a] Established dyes presented for comparison. Note that FITC is not a molecular rotor.

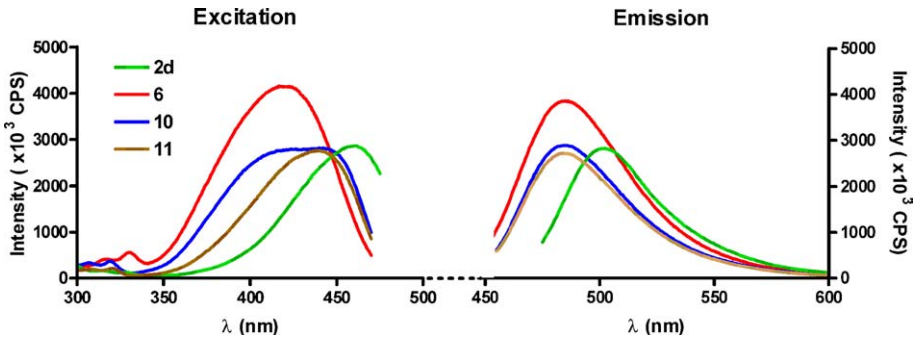

Fig. 2. Excitation and emission spectra of selected molecular rotors (**2d**, **10**, and **11**) in comparison to the established dye CCVJ (**6**).

and fell out of solution. In addition, **2b** exhibited rapid fluorescence decay (photobleaching) under the microscope.

3.4. Viscosity sensitivity

All dyes examined in this study exhibited an increase of emission intensity in solutions of increased viscosity. To determine the individual dye's viscosity sensitivity, mixtures of ethylene glycol and glycerol were used to modulate solvent viscosity. By plotting the maximum spectral intensity over the solvent viscosity in a double-logarithmic scale, it was possible to determine the power-law relationship between intensity and viscosity. Representative curves for dyes **2d**, **6**, **10**, and **11** can be seen in Fig. 3, and Table 2 lists the slopes together with the regression parameters for all dyes.

Viscosity-sensing performance was also tested in aqueous solutions of a high molecular-weight colloid, dextran. Viscosity sensitivity of **6** in such aqueous colloid

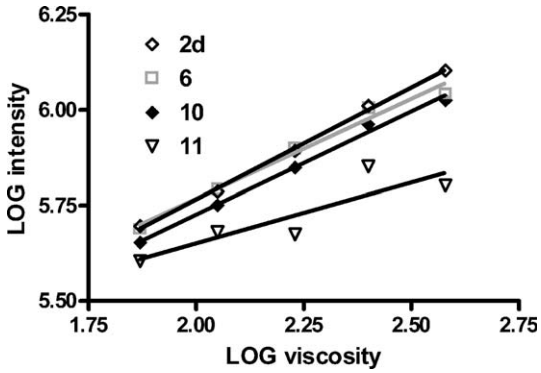

Fig. 3. Graphs showing the peak emission intensity over the solvent viscosity in a double-logarithmic scale for selected molecular rotors (**2d**, **10**, and **11**) in comparison to the established dye CCVJ (**6**). It can be seen that the values lie on a straight line, confirming the power-law relationship of intensity with viscosity.

Table 2
Regression results of log intensity over log viscosity to determine the exponent x in Eq. (2)

Dye	Regression slope (exponent x)	r^2	P
2b	0.3	0.81	0.036
2c	0.61	0.99	<0.0001
2d	0.59	0.99	<0.0001
10	0.54	0.99	0.0002
11	0.32	0.77	<0.05
6[a]	0.52	0.98	0.0014

[a] Established dye presented for comparison.

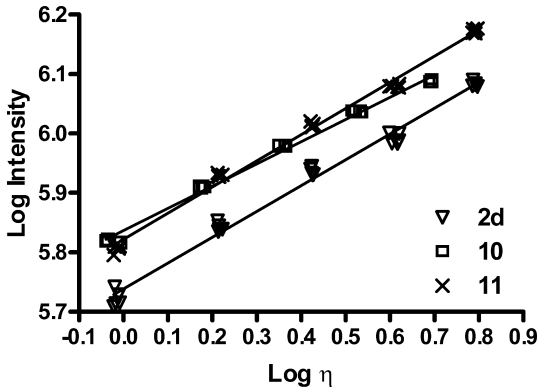

Fig. 4. Graphs showing the peak emission intensity in aqueous solutions of dextran at different concentrations. Shown is the intensity over the solvent viscosity in a double-logarithmic scale for selected molecular rotors (**2d**, **10**, and **11**). Similar to the behavior in ethylene glycol–glycerol mixtures, these probes exhibit power-law relationship between intensity and viscosity in aqueous colloid solutions.

systems has been established recently [29]. The new water-soluble dyes, **2d**, **10**, and **11**, underwent testing in water/dextran solutions. Fig. 4 shows the intensity increase with increasing concentration of dextran. The power-law relationship can again clearly be seen. The slopes in the double-logarithmic plot were found to be 0.44 ($r^2 = 0.99$, **2d**), 0.37 ($r^2 = 0.99$, **10**), and 0.44 ($r^2 = 0.99$, **11**). While the slopes were significantly different from zero in all cases with $P < 0.0001$, they were markedly lower than in the ethylene glycol/glycerol mix.

3.5. Sensitivity towards changes in the pH of the environment

Since these dyes are targeted at aqueous solutions, possibly at biological fluids with varying acidity, the influence of the solvent pH on the emission intensity was examined. As can be seen in Fig. 5, the dyes examined showed little variation of the emission intensity with pH in the pH range from 4.0 to 12.0. In the pH range from 3.0 to 9.0, **2d** shows no correlation ($r^2 = 0.05$, $P = 0.3$, not significant) between pH and intensity, while a slight positive correlation was found in **6** ($r^2 = 0.4$, $P = 0.002$). In more acidic solutions, the dyes precipitate, and a red-shift of the absorbance

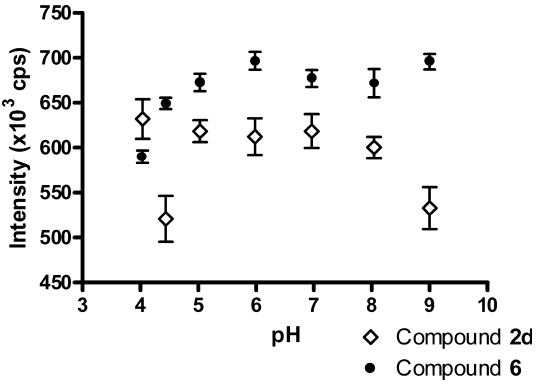

Fig. 5. Dependency of two selected dyes, **2d** and **6** of the pH value of the aqueous environment. Shown is the mean and SD of three independent measurements.

maximum takes place. In basic solutions of pH 10 and above, some quenching takes place in **2d**, while **6** remains pH-insensitive up to pH 12 (data not shown).

4. Discussion

Molecular rotors are a group of fluorescent molecules that are characterized by a dual deexcitation pathway. Molecular rotors in the excited singlet state can return to the ground state either through fluorescence emission or though the rotation of one molecule's subunit against the other around a single bond. Due to the ability to perform intramolecular rotation those molecules are also known as twisted intramolecular charge transfer (TICT) complexes. Since fluorescence emission and intramolecular rotation are competitive processes, the fluorescence quantum yield Φ depends strongly on the intramolecular rotation rate (Eq. (1)),

$$\Phi = \frac{k_r}{k_r + k_{nr}}, \tag{1}$$

where k_r is the radiative relaxation rate and k_{nr} the non-radiative (rotational) relaxation rate. When first discovered, TICT molecules such as 4-dimethylaminobenzonitrile (DMABN) were of high relevance because the intramolecular rotation rate depends on the polarity of the solvent [30]. Some molecular rotors are less polarity sensitive; primary determinant of intramolecular rotation and thus the quantum yield is the solvent's viscosity. The relationship has first been described by Förster and Hoffmann [23] following Eq. (2),

$$\log \Phi = C + x \cdot \log \eta, \tag{2}$$

where η is the solvent viscosity, x is a dye-dependent constant, and C is a temperature-dependent constant. While changes in the solvent's polarity causes a change in the Stokes shift, the emission intensity depends on the solvent viscosity. Those molecules have received increasing attention as microviscosity sensors in polymerization

processes [26], viscosity indicators in phospholipid bilayers and the cell membrane [24,31] and to measure biofluid viscosity in a non-mechanical manner [32]. The last application is of particular relevance, because traditional mechanical measurement of fluid viscosity is a time-consuming process, suffers from protein deposition at the instrument walls and from artefacts caused by protein crosslinking at the fluid–air interface. Recent studies indicate that fluorescence-based measurement of fluid viscosity with the precision of mechanical instruments is feasible. In addition, microscopic measurement of a rotor's fluorescence emission allows microviscosity measurement with high spatial resolution. Readily available molecular rotors, with the exception of CCVJ, are insoluble in water. For the determination of viscosity or microviscosity in aqueous environments it is therefore desirable to endue rotor derivatives that are readily soluble in water and aqueous liquids. In this study, we presented several new fluorescent molecules with rotor characteristics that are soluble in water and aqueous solutions.

Due to the constant C in Eq. (2), which reflects complex external influences, absolute viscosity measurement is not directly possible. Relative viscosity changes, for example the ratio of viscosities before and after a stimulus (η_1 and η_2, respectively), can be computed quantitatively from the corresponding peak intensities I_1 and I_2 using Eq. (3) under the assumption that C does not change during the experiment [4]:

$$\frac{\eta_1}{\eta_2} = \left(\frac{I_1}{I_2}\right)^{1/x}. \tag{3}$$

The constituents of complex fluids, for example, dextran or proteins, also influence the constants in Eq. (2). It is possible to calibrate the fluorescence-based viscosity measurement using similar fluids with known viscosity [29,32], but individual calibrations need to be performed for different compositions. For example, different calibration curves were found in aqueous solutions of dextran and hydroxyethylstarch probed with **6** [29]. Depending on the fluid, chemical interaction with the constituents cannot be fully excluded.

All new compounds exhibited spectral properties closely related to **1** and **6**. Absorption took place in the blue range between 420 and 460 nm, and light is emitted in the green range, generally between 480 and 510 nm. The Stokes shift was typically 40 nm. A trend can be seen that julolidine-based dyes (primarily **2c** and **2d**) are closely related to **1**, while single-ring structures (**10**, **11**) showed a blue-shift of the excitation peak over **1**, and a less pronounced shift of the emission peak towards the blue. The single-ring structure shows some similarity to the well-explored 4-(*N*, *N*-dimethylamino)-benzonitrile (DMABN), which is excited at 267 nm in the UV range and which emits blue light. While DMABN is primarily known for its TICT-induced second fluorescence band in polar solvents [30], the compounds described in this paper are primarily aimed at quantum yield changes with the viscosity of the environment. In environments of different polarity, only minor spectral shifts of less than 5 nm were seen (data not shown). Minor excitation blue-shifts were also noted at high dye concentrations above 25 μM. We attribute this to dye agglomeration, which shields some of the dye from the polar environment. This effect defines an upper concentration limit for the use of these dyes. Dye **10** exhibits a relatively large

plateau in the excitation spectrum. Most likely this is caused by a double absorption maximum, similar to the ones found in related dyes [28], but more closely spaced so that the peaks are indistinguishable.

All dyes exhibited increased emission intensity in viscous fluids as can be expected from viscosity-sensitive molecular rotors. In a standard experiment [33], mixtures of ethylene glycol and glycerol were used to modulate viscosity over a wide range (from 14 mPa s for pure ethylene glycol up to approximately 800 mPa s for pure glycerol) without significantly changing the solvent's polarity. As shown in Table 2 and Fig. 3, the dyes presented in this study exhibited similar behavior, a power-law relationship between intensity and viscosity that is well described by Eq. (2). Two empirical constants exist in Eq. (2), the dye-dependent constant x [23] and the constant C that is temperature-dependent. In our experiments we assumed a proportional relationship of the measured peak emission intensity I with the quantum yield Φ, where the proportionality is determined by such factors as excitation light intensity, geometry, and detector efficiency. These external influences can be factored into a modified constant C, allowing to determine x from the slope of intensity over viscosity in double-logarithmic scale. This constant x can be interpreted as the dye's sensitivity towards viscosity, because higher values of x amplify the intensity increase with viscosity. Dyes **2c**, **2d**, and **10** exhibited the highest values for x, all of them very close to the theoretical value of 0.6 expected for DCVJ (**1**) [23]. The primary cause for lower values of x in dyes **2b** and **11** was a saturation effect at high viscosities, where intensity no longer followed the power-law relationship at the highest viscosity. This effect led to both reduced slope x and relatively poor regression data in the double-logarithmic fit, and potentially puts an upper limit to the viscosity that can be sensed to around 500 mPa s. For comparison, full blood viscosity is approximately 5.7 mPa s, ethylene glycol 14 mPa s, and glycerol above 850 mPa s.

Different mechanisms were employed to make the dyes hydrophilic. While **2c** and **2d** build on ethylene glycol to achieve hydrophilic properties, **10** presents hydroxyl groups to the environment, and **2b** features a COOH group much like **6**. In the case of dye **11**, which does not have polar groups, the substitution of the tricyclic structure for a single ring and an alkyl group was sufficient to ensure solubility. This effect was not observed in a comparable julolidine-based methyl ester (**2e**), which was tried elsewhere [28] and found insoluble in water.

Since this study was aimed at the synthesis of molecular rotors that may act as viscosity sensors in aqueous solutions, viscosity sensitivity was verified in water–colloid systems similar to **6** as described in [29]. Dextran is a large starch molecule that can be used in different concentrations to increase the viscosity of aqueous solutions. Dyes with high water solubility, **2d**, **10**, and **11**, exhibit power-law relationship between peak emission intensity and dextran-modulated viscosity. Compared to mixtures of ethylene glycol and glycerol, however, the slope x was markedly lower. This is consistent with findings using **6** [29], where dextran solutions exhibited the lowest slope among different starches. We hypothesize that this behavior may be caused by direct non-covalent interaction of the dye with hydrophobic sections of the starch molecules, an effect that would withdraw some of the dye from the free-volume interaction required for the viscosity-sensing process.

Intensity was compared with mechanical viscosity data. These measurements are different primarily because the fluid is sheared to obtain its viscosity in the rheometer, while no shear is applied when measuring fluorescence. This needs to be taken into account, because some fluids (particularly solutions of macromolecules) may exhibit non-Newtonian behavior. In our experiments, mixtures of ethylene glycol and glycerol were considered Newtonian, while dextran solutions showed some shear-thinning. Viscosity values were taken at a point where an increase of shear rate showed no further reduction in the apparent viscosity. Thus, fluorescence emission intensity was correlated to asymptotic viscosity. The fundamental relationship between intensity and viscosity, however, would not be changed for other viscosity points, e.g., extrapolated values at zero shear rate. Only the constant C in Eq. (2) would change, corresponding to a parallel shift of the regression line in the double-logarithmic plot.

Compound **10** and its precursors, **8** and **9**, are chiral. In this study, they have been synthesized as racemic mixture but the presented synthesis can be used to obtain enantiomerically pure forms. Since most biological environments, for example, dextran solutions, the cytosol, cell membranes, are chiral, it is conceivable that the two antipodes of **10** could offer additional information about a possible enantiospecific nature of viscosity in biological media.

An important result that has not yet been extensively reported is the dye behavior in solutions of different pH. If molecular rotors are to be used as viscosity sensors in biofluids, the influence of proton concentration on the emission intensity in the physiological range should be known. Our data indicate that in the range from pH 4 to pH 10, only small intensity variations can be observed. Deviations remain within +7/−11% of the average intensity. No statistically significant trend can be seen in **2d**. In even more acidic solutions, however, several effects can be observed. A spectral red-shift and reduced intensity (**6**) indicates energy loss by solvent interaction as well as quenching by protonation. Solubility is also reduced, preventing solutions of concentrations higher than 1 μM. It can be concluded, however, that in the physiological range centered on pH 7.5, pH influences do not play a significant role.

5. Conclusion

In this paper we introduced several new molecular rotors aimed at aqueous solutions, and demonstrated how twisted intramolecular charge transfer complex molecules can be designed from a julolidine group and different polar groups that ensure solubility. Of the several compounds tested, **2d** and **10** were of particular interest with a combination of high viscosity sensitivity (high exponent x in Eq. (2)), high solubility in water, and demonstrated sensitivity to viscosity in aqueous colloid solutions. Up to this point, most molecular rotors, namely the well-known DCVJ (**1**), were insoluble in water. The fundamental difference between **6** and the new dyes **2d** and **10** is the absence of a carboxyl group. While **2d** builds on ethylene glycol to achieve hydrophilic properties, **10** presents hydroxyl groups to the environment. These differences may be exploited to allow or disallow specific reactions with the solvent, such

as ester formation. These dyes show promise for use as hydrophilic viscosity sensors in biofluids, such as blood plasma and mixtures of plasma and colloids [32]. Future studies may involve a covalently bound fluorescent non-rotor unit to serve as a reference, leading to a ratioing dye that eliminates sample influences and facilitates calibration.

Acknowledgments

We gratefully acknowledge financial support through NIH Grant 1R21-RR018399. We thank the reviewers for helpful comments, particularly the question of calibrating the intensity measurements, and the note on the additional use of the enantiomers of **10**.

References

[1] W. Möller, S. Takenaka, M. Rust, W. Stahlhofen, J. Heyer, J. Aerosol. Med. 10 (1997) 171–186.
[2] T.P. Stossel, Science 260 (1993) 1086–1094.
[3] P.F. Davies, Physiol. Rev. 75 (1995) 519–560.
[4] M.A. Haidekker, N. L'Heureux, J.A. Frangos, Am. J. Physiol. Heart Circ. Physiol. 278 (2000) H1401–H1406.
[5] D.B. Goldstein, Annu. Rev. Pharmacol. Toxicol. 24 (1984) 43–64.
[6] R.A. Harris, R.J. Hitzemann, Curr. Alcohol 8 (1981) 379–404.
[7] R.A. Harris, P. Bruno, J. Neurochem. 44 (1985) 1274–1281.
[8] D.A. Johnson, R. Cooke, H.H. Loh, Adv. Exp. Med. Biol. 126 (1980) 65–68.
[9] G. Deliconstantinos, V. Villiotou, J.C. Stavrides, Biochem. Pharmacol. 49 (1995) 1589–1600.
[10] M.M. Gleason, M.S. Medow, T.N. Tulenko, Circ. Res. 69 (1991) 216–227.
[11] O. Nadiv, M. Shinitzky, H. Manu, D. Hecht, C.T. Roberts Jr., D. LeRoith, Y. Zick, Biochem. J. 298 (Pt. 2) (1994) 443–450.
[12] W. Osterode, C. Holler, F. Ulberth, Diabet. Med. 13 (1996) 1044–1050.
[13] M. Shinitzky, Biochim. Biophys. Acta 738 (1984) 251–261.
[14] J. Harkness, Biorheology 8 (1971) 171–193.
[15] R.L. Letcher, S. Chien, T.G. Pickering, J.E. Sealey, J.H. Laragh, Am. J. Med. 70 (1981) 1195–1202.
[16] M.A. McGrath, R. Penny, J. Clin. Invest. 58 (1976) 1155–1162.
[17] D.O. Bates, J.R. Levick, P.S. Mortimer, Clin. Sci. (Lond.) 85 (1993) 737–746.
[18] H. Schad, H. Brechtelsbauer, Z. Lymphol. 10 (1986) 14–19.
[19] M. Intaglietta, Artif. Cells Blood Substit. Immobil. Biotechnol. 22 (1994) 137–144.
[20] H.H. Lipowsky, J.C. Firrell, Am. J. Physiol. 250 (1986) H908–H922.
[21] A.G. Tsai, M. Intaglietta, Biorheology 38 (2001) 229–237.
[22] G.R. Cokelet, in: Y.C. Fung, N. Perrone, M. Anliker (Eds.), Biomechanics—Its Foundations and Objectives, Prentice-Hall, Englewood Cliffs, 1972, pp. 63–103.
[23] Th. Förster, G. Hoffmann, Z. Phys. Chem. 75 (1971) 63–76.
[24] C.E. Kung, J.K. Reed, Biochemistry 25 (1986) 6114–6121.
[25] R.O. Loutfy, B.A. Arnold, J. Phys. Chem. 86 (1982) 4205–4211.
[26] R.O. Loutfy, Pure Appl. Chem. 58 (1986) 1239–1248.
[27] M. Haidekker, T. Brady, K. Wen, C. Okada, H. Stevens, J. Snell, J. Frangos, E. Theodorakis, Bioorg. Med. Chem. 10 (2002) 3627–3636.
[28] M.A. Haidekker, T. Ling, M. Anglo, H.Y. Stevens, J.A. Frangos, E.A. Theodorakis, Chem. Biol. 8 (2001) 123–131.
[29] W. Akers, M.A. Haidekker, J. Biomech. Eng. 126 (2004) in press.

[30] Z.R. Grabowski, J. Dobkowski, Pure & Appl. Chem. 55 (1983) 245–252.
[31] M.L. Viriot, M.C. Carré, C. Geoffroy-Chapotot, A. Brembilla, S. Muller, J.-F. Stoltz, Clin. Hemorheol. Microcirc. 19 (1998) 151–160.
[32] M.A. Haidekker, A.G. Tsai, T. Brady, H.Y. Stevens, J.A. Frangos, E. Theodorakis, M. Intaglietta, Am. J. Physiol. Heart Circ. Physiol. 282 (2002) H1609–H1614.
[33] T. Iwaki, C. Torigoe, M. Noji, M. Nakanishi, Biochemistry 32 (1993) 7589–7592.